SUPPLEMENTARY MATERIAL

Multiplexed immunofluorescence delineates proteomic cancer cell states associated with metabolism

Authors: Anup Sood[7]*, Alexandra M. Miller[2]*, Edi Brogi[3]*, Yunxia Sui[7], Joshua Armenia[1,] Elizabeth McDonough[7], Alberto Santamaria-Pang[7], Sean Carlin[4], Aleksandra Stamper[1], Carl Campos[1], Zhengyu Pang[7], Qing Li[7], Elisa Port[5,†], Tom Graeber[8], Nikolaus Schultz[1,6], Fiona Ginty[7,#], Steven M. Larson[4,#], and Ingo K. Mellinghoff [1,2,9,#]

Affiliations: [1] Human Oncology and Pathogenesis Program, and the Departments of [2]Neurology, [3]Pathology, [4]Radiology, [5]Surgery, and [6]Epidemiology and Biostatistics, Memorial Sloan-Kettering Cancer Center, New York, NY10065, USA; [7]Diagnostic Imaging and Biomedical Technologies, General Electric Global Research Center, Niskayuna, NY 12309; [8]Department of Molecular and Medical Pharmacology, University of California at Los Angeles, CA 90095; [9]Department of Pharmacology, Weill-Cornell Medical School, New York, NY10021, USA

* Equal contribution. # To whom correspondence should be addressed: ginty@research.ge.com, LarsonS@mskcc.org, and mellingi@mskcc.org; † Present Addresses: Department of Surgery, Mount Sinai Hospital, New York, NY10029

Index

Supplementary Figure 1

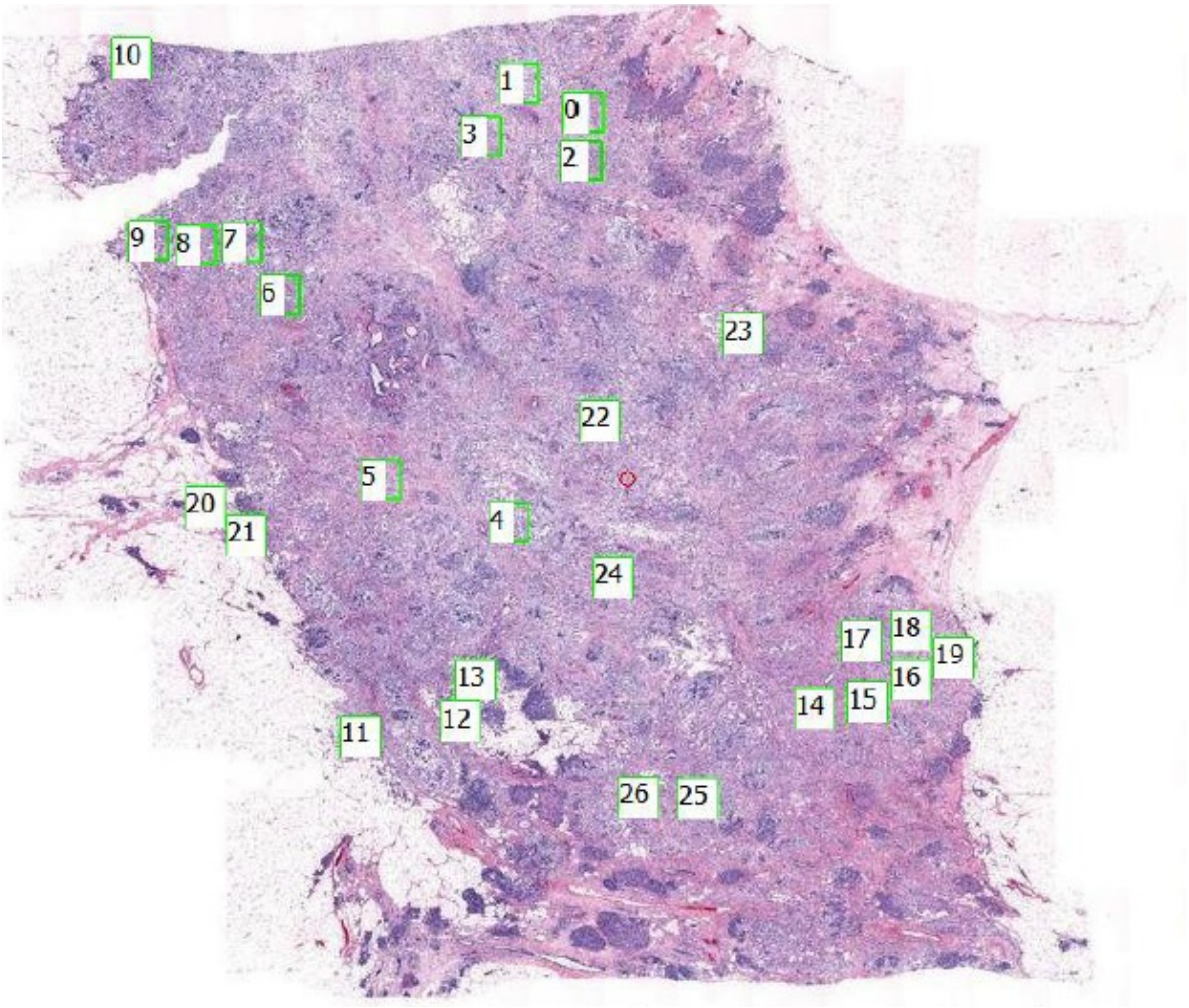

Supplementary Figure 1. Placement of 10- 40 Fields-of-View (FOVs) per tumor specimen. Shown is a virtual hematoxylin/eosin (H&E) image of one human breast cancer specimen (#068). Each green box indicates one FOV.

Supplementary Figure 2

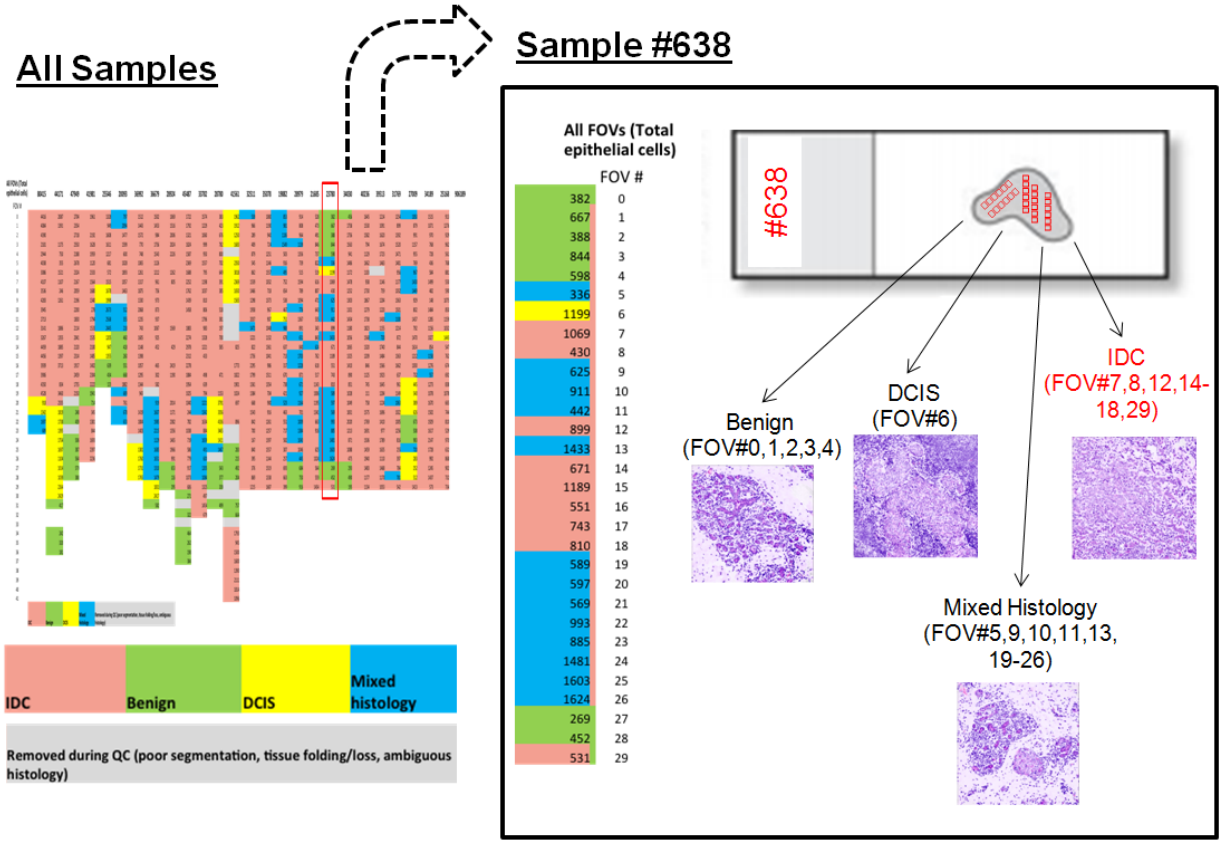

Supplementary Figure 2. Pathological Annotation of all FOVs. The left part of the figure shows an overview of the data presented in Supplementary Table 3 at higher resolution. Each column represents one tumor specimen, each row represents one FOV. For each tumor sample, exemplified by tumor #638 in the right part of the figure, 10-40 fields-of-view (FOVs) were placed, reviewed by a breast cancer pathologist (E.B.), and classified into one of four categories: IDC (red), benign tissue (green), ductal carcinoma-in-situ (DCIS, yellow), or mixed histology (blue). The right part of the figure shows the distribution of all FOVs amongst the four histopathological categories (Sample #638). In tumor #638, FOVs #0/1/2/3/4 contained mostly non-malignant epithelial cells (benign breast tissue), whereas FOVs #7, 8, 12, 14-18, and 29 consisted mostly of invasive ductal carcinoma cells. **Note,** the majority of FOVs in our dataset represented IDC (red cells in left part of figure). FOVs representing benign breast tissue (green), DCIS (yellow), or areas of mixed histology (blue) were excluded from the analysis of protein expression clusters. The numbers listed in each cell represent the number of epithelial cells in each FOV.

Supplementary Figure 3

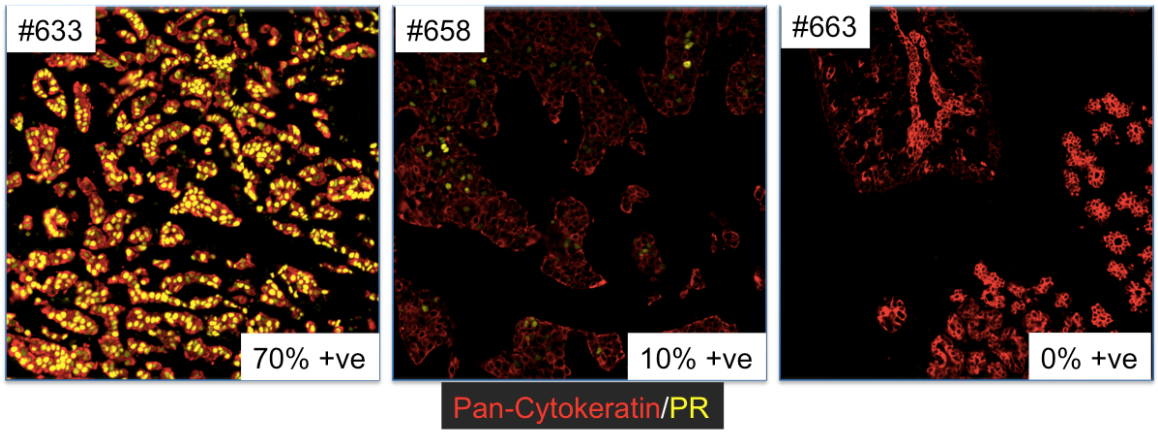

Supplementary Figure 3. Progesterone Expression in three representative breast cancers (#633, #658, #663). Pancytokeratin=red. PR=yellow. Sample #658 was one of the samples that was discordant between the CLIA result and the IF results. Magnification=20x.

Supplementary Figure 4:

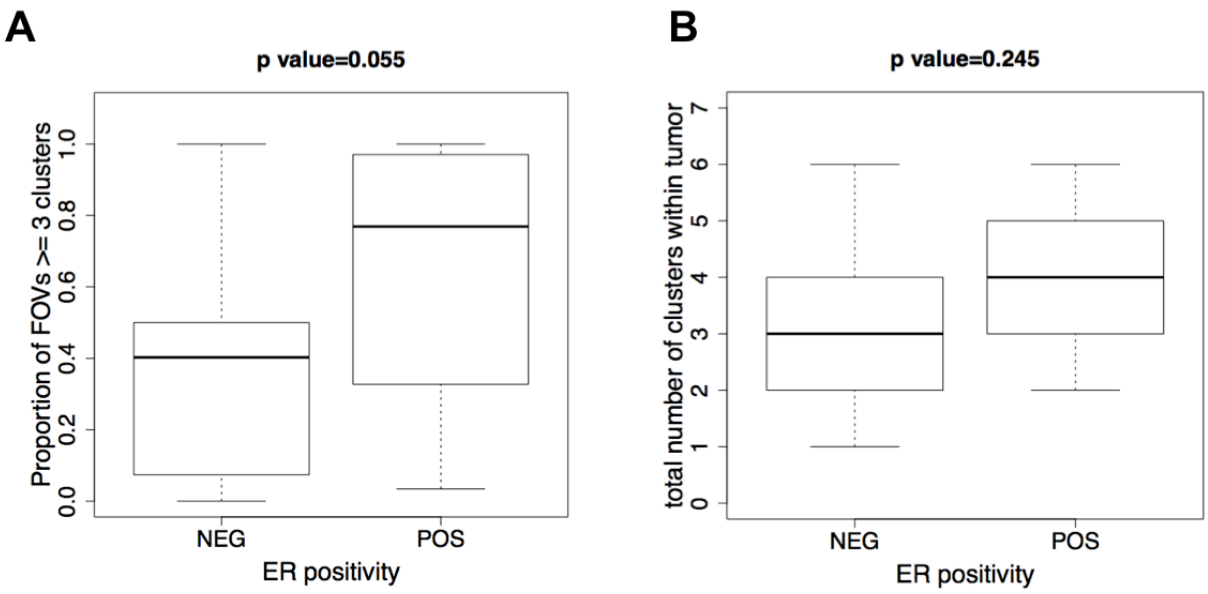

Supplementary Figure 4. Relationship between ER status and heterogeneity in protein expression. There was a trend toward higher intratumoral heterogeneity in ER-positive tumors, but this relationship was not significant when heterogeneity was defined as **A.)** the fraction of FOVs containing three of more different protein expression clusters (p=0.06, t-test) or **B.)** the number of clusters expressed in > 1 % of neoplastic cells (p=0.25, t-test).

Supplementary Figure 5:

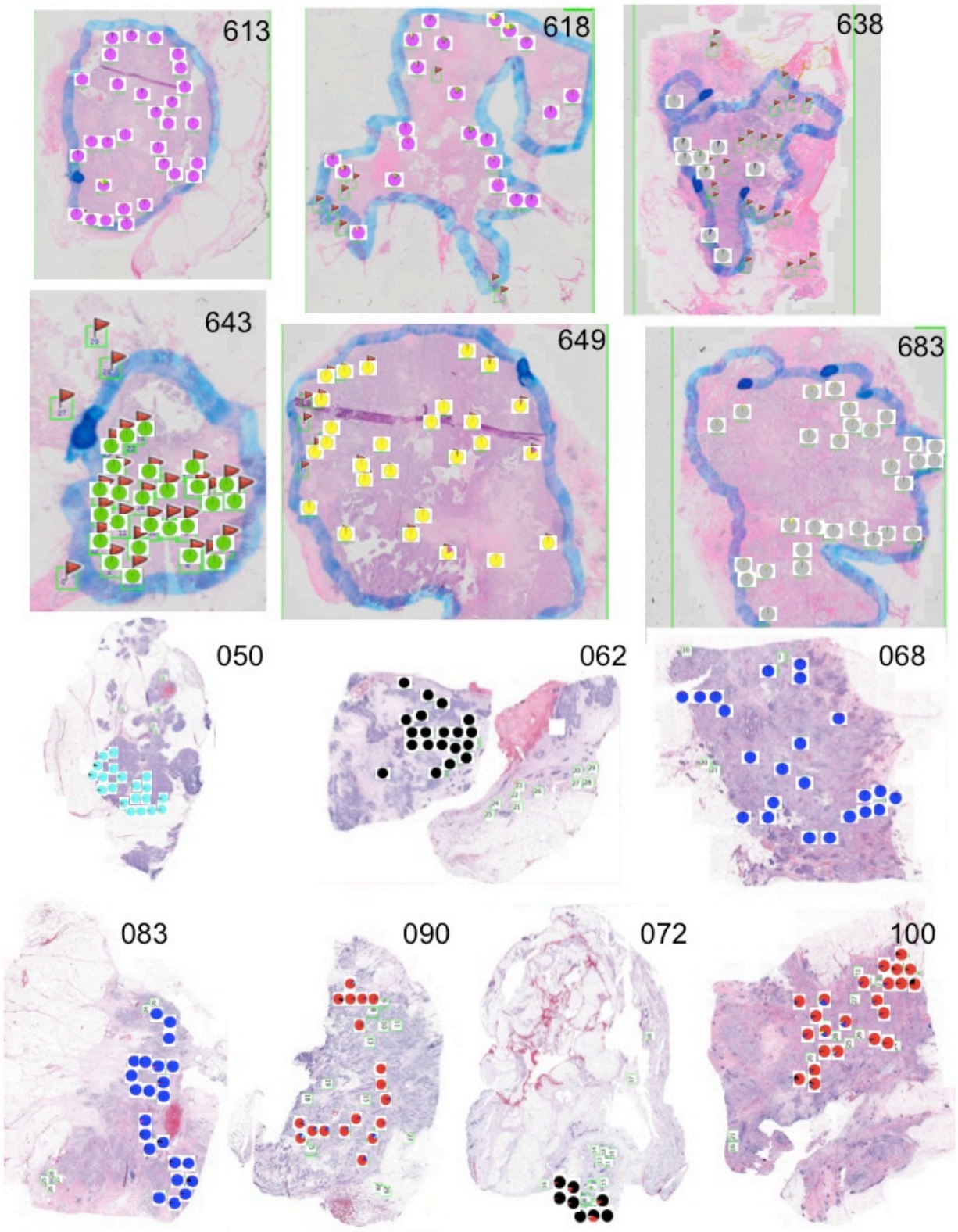

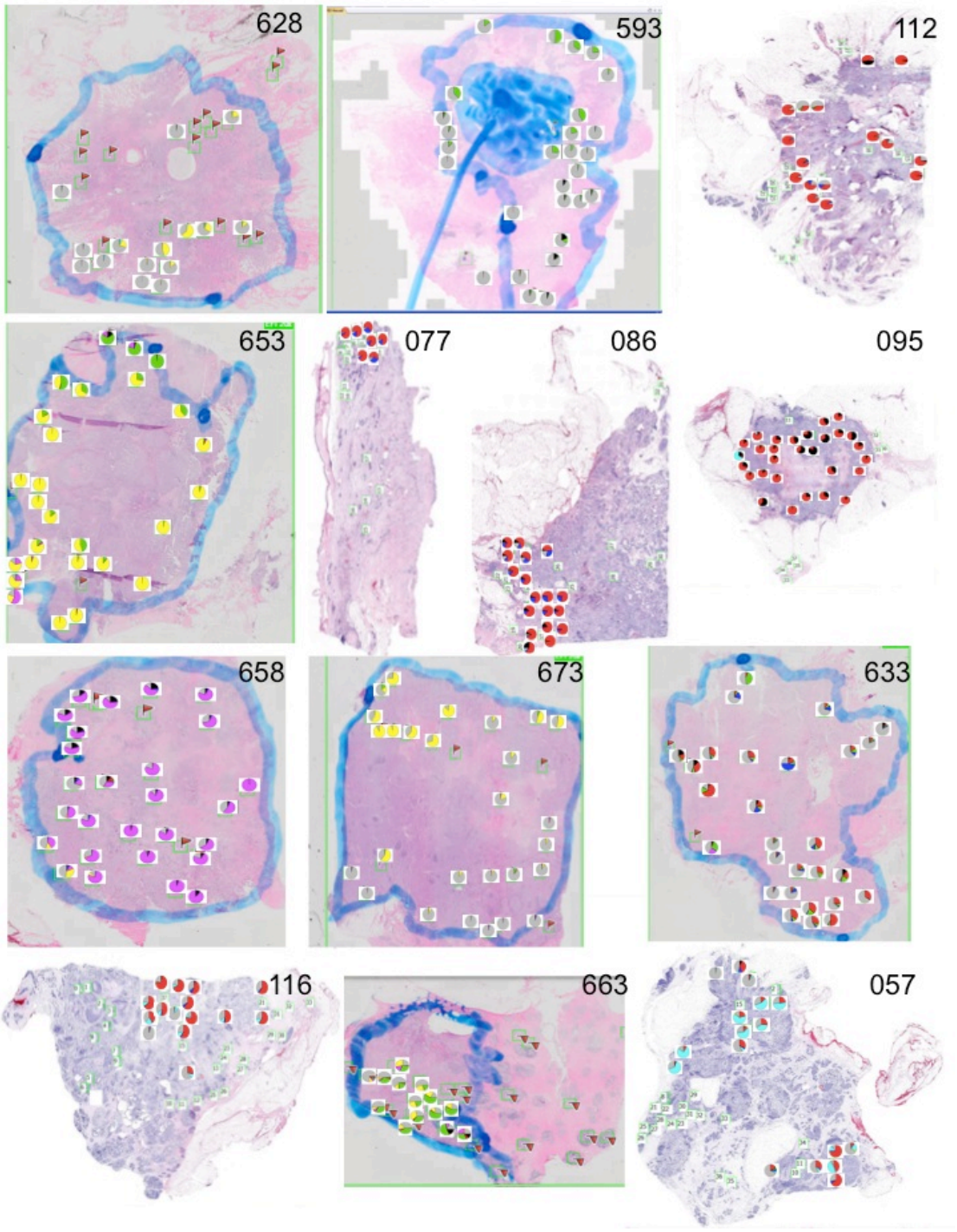

Supplementary Figure 5. Spatial Distribution of Protein Expression Clusters. Shown are low resolution images of each breast cancer specimen. Colored pie charts show the distribution of protein expression clusters within each FOV (cluster color identical to Figure 4 in main MS). Green boxes without pie charts represent FOVs that were not included in our quantitative analysis of protein expression because they included areas of mixed histology, ductal carcinoma-in-situ, or normal epithelial cells.

Supplementary Figure 6

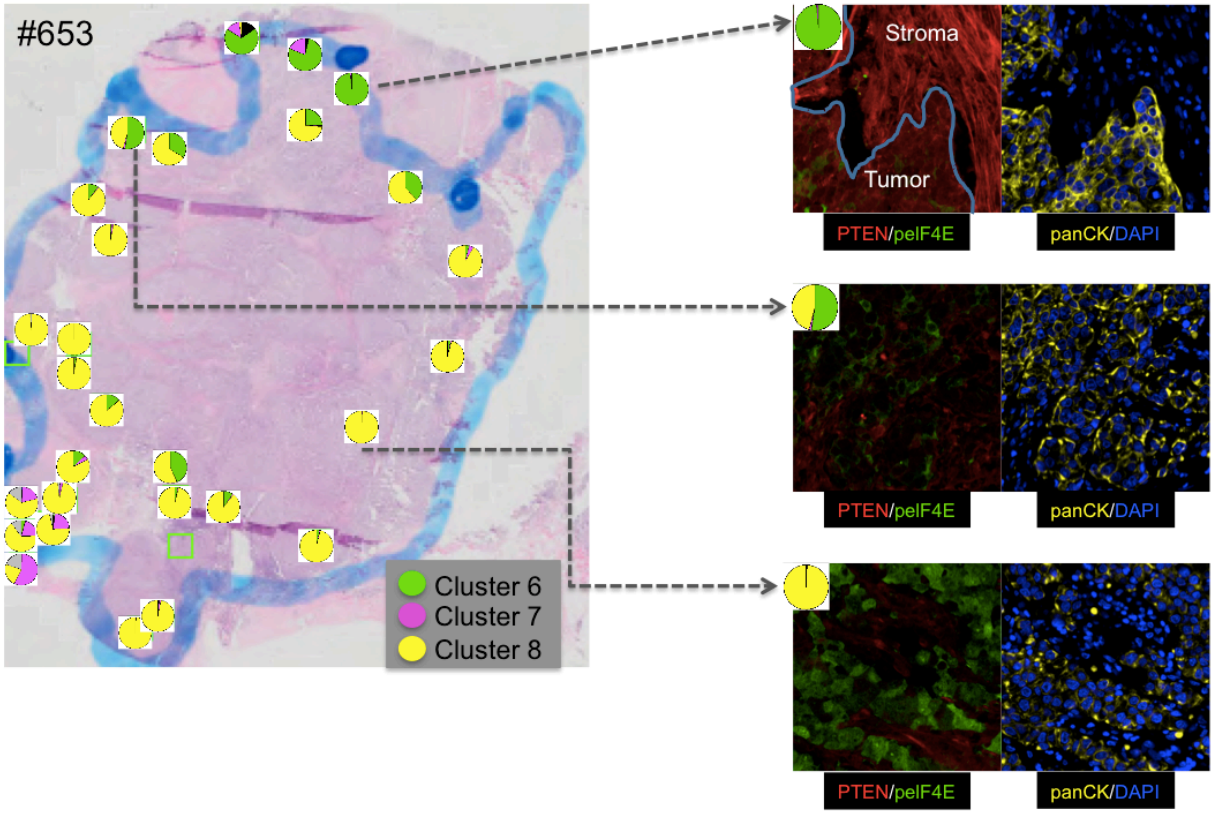

Supplementary Figure 6: Regional Loss of PTEN expression in tumor # 653. Left Panel: Low resolution view of the entire section of tumor #653. Colored pie charts show the distribution of protein expression clusters within each FOV. Note, that the upper portion of the tumor section 653 is characterized predominantly by cluster 6 cells. There is a transitional zone that is heterogeneous in which there is a mixture of cluster 6 and cluster 8 positive cells, then in the lower portion of the tumor, the cells mostly belong to cluster 8. Right Panel: Immuno-fluorescence staining for the indicated FOVs. PTEN (red) is strongly expressed in the upper region of the tumor (both stroma and tumor cells). In the lower region, PTEN expression is only noted in panCK (yellow)-negative stromal cells, but not panCK-positive tumor cells. Additionally, note increase staining for p-eIFAE (green) in PTEN negative tumor cells. DAPI=blue. Magnification=20x; Zoom=3x.

Supplementary Figure 7:

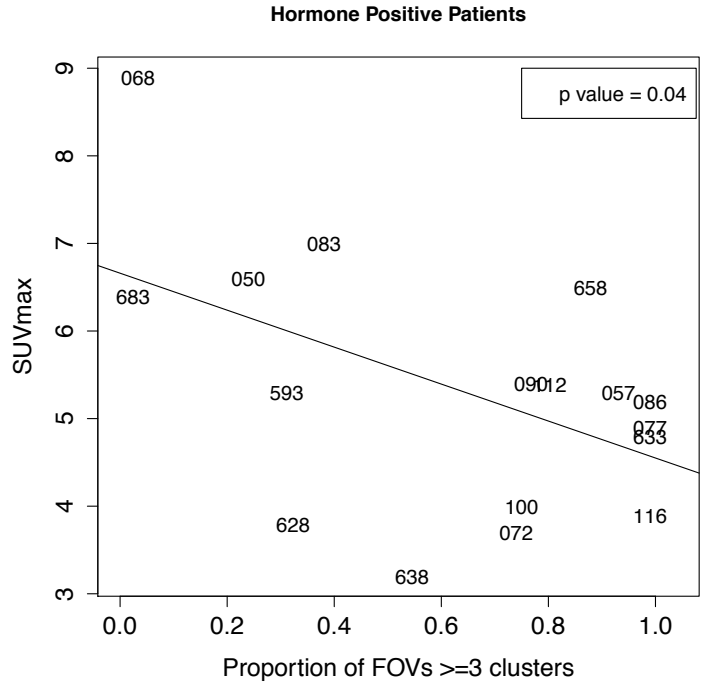

Supplementary Figure 7: Relationship between intratumoral heterogeneity and FDG-uptake in ER positive tumors. A linear regression model was used to compare intratumoral heterogenetity with SUVmax. Heterogeneity was defined as the fraction of FOVs containing three or more distinct protein expression clusters. The FOVs were binned into “homogenous” vs. “heterogeneous” using a cut-off of >=3 clusters (the linear slope is -2.11 with p=0.04 based on t-test).

Supplementary Figure 8:

Univariate Analysis

Predictor of FDG SUV max	P-value	Slope
Negatively correlated		
ER (mean)	4.03E-06	-2.26
PR (mean)	2.37E-03	-1.29
PTEN (mean)	4.17E-02	-4.06
Positively Correlated		
Ki67 (mean)	6.57E-03	4.89
N-myc downstream regulated 1 (std. dev.)	1.62E-03	6.71
Glut1 (Mean)	1.42E-02	1.81

Multivariate Analysis

Predictor of FDG SUV max	Regression co-efficient	p-Value
(Intercept)	12.67	1.12E-**04**
ER (mean)	-1.75	6.38E-05
PR (mean)	-0.36	2.26E-01
N-myc downstream regulated 1 (std. dev.)	3.86	9.59E-03

Supplementary Figure 8. Relationship between individual protein markers and tumor uptake of FDG. A.) Univariate Analysis. Slope represents predicted change in SUVmax per log2 unit change in corresponding biomarker metric. **B.)** Multivariate analysis.

Supplementary Figure 9:

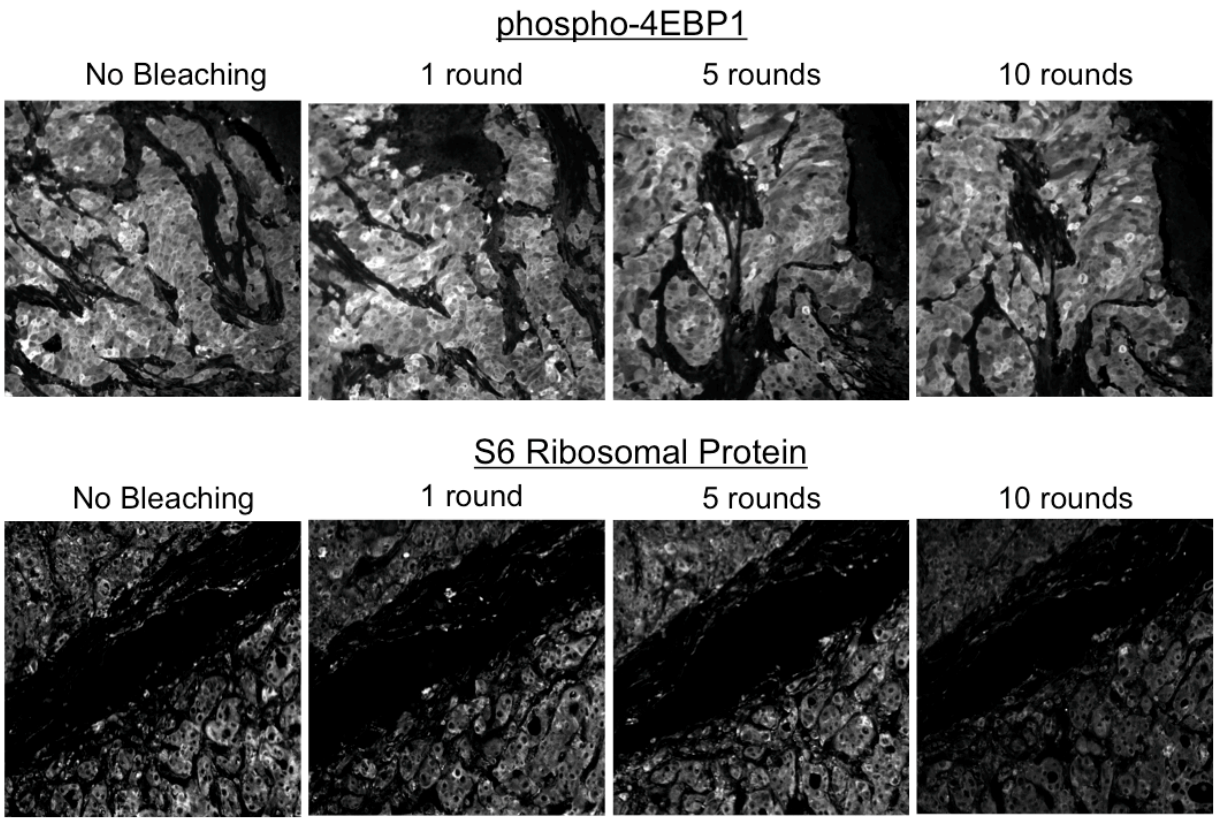

Supplementary Figure 9: Effect of sequential dye inactivation cycles on different protein antigens. Top tier: phospho-4EBP1 staining, bottom tier: S6 Ribosomal Protein. Please see Text for details. Magnification=20x; Zoom=2x.

Supplementary Table 1:

Biomarker	Vendor	Cat#	Clone
AR	Dako	M3562	AR441
4EBP1 (pT37/pT46)	Cell Signaling	2855B	236B4
Cadherin-pan	Neomarkers	RB-9036	polyclonal
CD31	Cell Signaling	3528	89C2
cMYC	Epitomics	1472	Y69
Cytokeratin_pan (PCK26)*	Sigma	C1801	PCK-26
Cytokeratin_pan (AE1)*	eBioscience	14-9001	AE1
EGFR (pY1068)	Epitomics	1727-1	EP774Y
EIF4E (pS209)	Epitomics	2227-x	EP2151Y
ER	Leica	PA0151	6F11
Erk1/2 (pT202/pY204)	Cell Signaling	4376BF	20G11
Glut-1	Millipore	07-1401	polyclonal
Her2	Cell Signaling	4290	D8F12
Histone H3 (pS10)	Millipore	09-797	polyclonal
HK2	Cell Signaling	2867	C64G5
IGF1R	Lifespan	LS-C82136	3C8B1
Ki67	Thermo Fisher	RB 1510 PABX	polyclonal
LDH-A	Cell Signaling	3582BF	C4B5
NaKATPase	Epitomics	2047-x	EP1845Y
p53	Dako	M7001	DO-7
PDK1 (pS241)	Abcam Epitomics	ab109460	EPR336(2)
PR	Dako	M3568	PgR1294
PTEN	Cell Signaling	9188	D4.3
S6	Cell Signaling	2217	5G10
S6 (pS235/pS236)	Cell Signaling	4858B	D57.2.2E
Transferrin Receptor I	Invitrogen	13-6800	EPR4013
NDRG1	AGI	S0731	H-90
CA9	Thermo Fisher	PA1-16592	D78A4

Supplementary Table 1: List of primary antibodies. * A cocktail of two in a 2:1 (PCK26:AE1) ratio was used to stain keratins for delineating epithelial region.

Supplementary Table 2:

Patient #	Histology	Age	Sex	Tumor Size (cm)	Histologic Grade	Nuclear grade	Lymph Node Involvement
593	IDC	64	F	2.0	III/III	III/III	YES
613	IDC	61	F	2.5	III/III	III/III	YES
618	IDC	57	F	4.0	III/III	III/III	YES
628	IDC	62	F	2.5	II/III	II/III	YES
633	IDC	69	F	4.2	III/III	III/III	YES
638	IDC	28	F	1.4	III/III	III/III	YES
643	IDC	44	F	1.3, 1.2	N/A	N/A	YES
649	IDC	29	F	2.3	II/III	III/III	YES
653	IDC	48	F	8.5	III/III	III/III	YES
658	IDC	28	F	3.2	III/III	III/III	NO
663	IDC	34	F	2.1	III/III	III/III	YES
673	IDC	46	F	3.5	III/III	III/III	YES
683	IDC	40	F	9.5	III/III	III/III	YES
050	IDC	31	F	N.D.	III/III	II/III	YES
057	IDC	38	F	2.3	III/III	II/III	NO
062	IDC	46	F	4	III/III	III/III	NO
116	IDC	34	F	1.7	III/III	II/III	YES
068	IDC	51	F	3.0	III/III	III/III	YES
072	IDC	71	F	1.2	III/III	II/III	YES
077	IDC	41	F	2.5	III/III	III/III	YES
083	IDC	46	F	3.5	III/III	III/III	YES
086	IDC	42	F	4.5	II/III	II/III	YES
112	IDC	39	F	8.0	III/III	III/III	YES
100	IDC	33	F	4.5	III/III	II/III	YES
095	IDC	60	F	1.8	III/III	III/III	YES
090	IDC	64	F	5.0	III/III	III/III	YES

Supplementary Table 2. Breast cancer patient clinico-pathologic characteristics (n=26). IDC, invasive ductal carcinoma; N.D. = not able to be determined; N.A. = not available. Tumor #643 had two foci.